research communications

Crystal structure refinement of magnesium zinc divanadate, MgZnV$_2$O$_7$, from powder X-ray diffraction data

Stephanie J. Hong, Jun Li* and Mas A. Subramanian

Department of Chemistry, Oregon State University, Corvallis, Oregon 97331, USA. *Correspondence e-mail: lijun@oregonstate.edu

The crystal structure of magnesium zinc divanadate, MgZnV$_2$O$_7$, was determined and refined from laboratory X-ray powder diffraction data. The title compound was synthesized by a solid-state reaction at 1023 K in air. The crystal structure is isotypic with Mn$_{0.6}$Zn$_{1.4}$V$_2$O$_7$ ($C2/m$; $Z = 6$) and is related to the crystal structure of thortveitite. The asymmetric unit contains two metal sites with statistically distributed magnesium and zinc atoms with the atomic ratio close to 1:1. One (Mg/Zn) metal site (M1) is located on Wyckoff position $8j$ and the other (M2) on $4h$. Three V sites (all on $4i$), and eight O (three $8j$, four $4i$, and one $2b$) sites complete the asymmetric unit. The structure is an alternate stacking of V$_2$O$_7$ layers and (Mg/Zn) atom layers along [20$\bar{1}$]. It is distinct from other related structures in that each V$_2$O$_7$ layer consists of two groups: a V$_2$O$_7$ dimer and a V$_4$O$_{14}$ tetramer. Mixed-occupied M1 and M2 are coordinated by oxygen atoms in distorted trigonal bipyramidal and octahedral sites, respectively.

1. Chemical context

Mixed vanadium oxides with tetrahedrally coordinated pentavalent vanadium ions have been used as catalysts in the heterogeneous oxidation process (Chang & Wang, 1988). Since there is a strong correlation between the crystal structure and its properties, the phase relations of vanadates have been thoroughly investigated. During the course of studying the phase diagram in the MgO–ZnO–V$_2$O$_5$ system, a new phase was identified by its X-ray diffraction pattern in the solid-solution range between (Mg$_{0.80}$Zn$_{1.20}$)V$_2$O$_7$ and (Mg$_{1.16}$Zn$_{0.84}$)V$_2$O$_7$, which was completely different from Mg$_2$V$_2$O$_7$ or Zn$_2$V$_2$O$_7$ (Chang & Wang, 1988). The crystal structure of the new phase has not been reported to date. We present here the crystal structure of MgZnV$_2$O$_7$ (Fig. 1), as determined and refined from laboratory powder X-ray diffraction data (Table 1).

2. Structural commentary

The crystal structure of magnesium zinc divanadate, MgZnV$_2$O$_7$, is isotypic with Mn$_{0.6}$Zn$_{1.4}$V$_2$O$_7$ (Knowles *et al.*, 2009), where statistically distributed Mg and Zn atoms (Mn and Zn for Mn$_{0.6}$Zn$_{1.4}$V$_2$O$_7$) are located in disordered environments in the crystal structure. The unit-cell volume of MgZnV$_2$O$_7$ is smaller than that of Mn$_{0.6}$Zn$_{1.4}$V$_2$O$_7$ by 1.65%.

The crystal structure of MgZnV$_2$O$_7$ is shown in Fig. 1a. There are (Mg1/Zn1) (on Wyckoff position $8j$, site symmetry 1), (Mg2/Zn2) (on $4h$, 2), three V (all on $4i$, m), and eight O
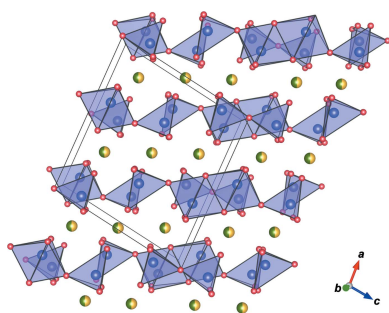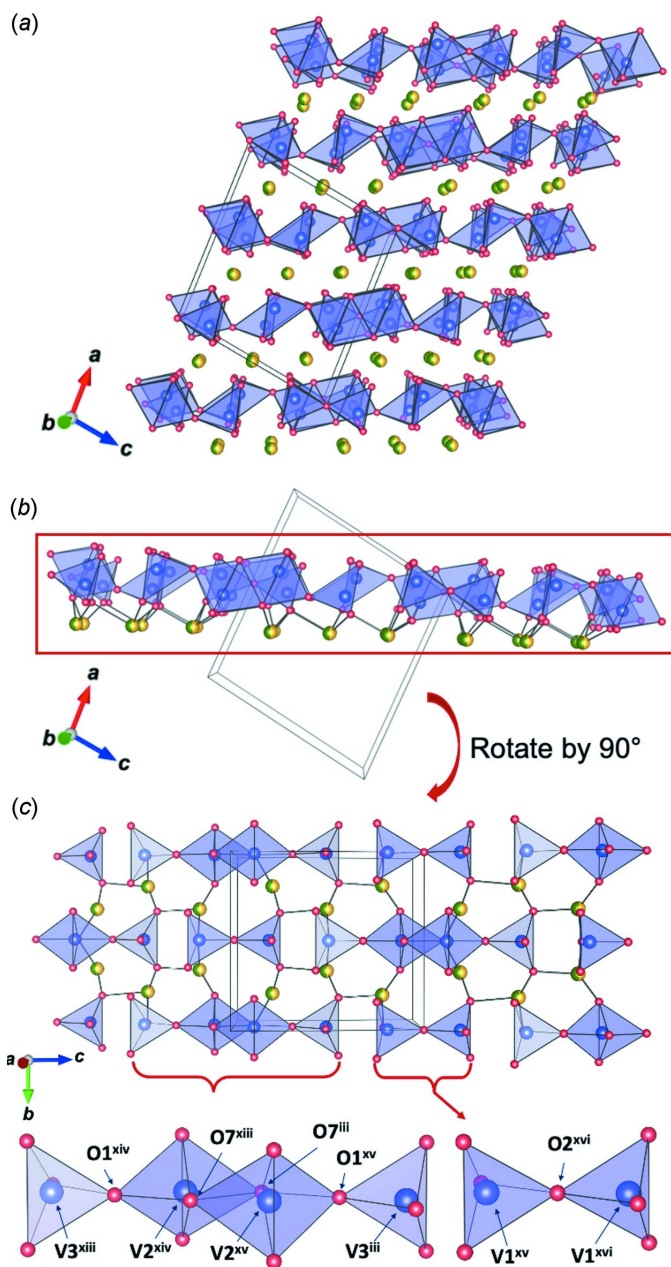
Figure 1
The crystal structure of MgZnV$_2$O$_7$ with VO$_4$ tetrahedra, VO$_5$ trigonal bipyramids (light purple), and (Mg/Zn) atoms (green/yellow). (*a*) overview of the structure, (*b*) a selected slab of one V$_2$O$_7$ layer and the adjacent (Mg/Zn) layer, and (*c*) a top view of the slab of (*b*) and magnified local structure of V$_4$O$_{14}$ tetrameric and V$_2$O$_7$ dimeric units. [Symmetry codes: (xiii) $-x + 1$, $-y + 1$, $-z$; (xiv) x, $y + 1$, $z - 1$; (xv) $-x + 1$, $-y + 1$, $-z + 1$; (xvi) $x + 1$, $y + 1$, $z + 1$.]

(three 8*j*, four 4*i*, and one 2*b*, 2/*m*) sites in the asymmetric unit, where (Mg1/Zn1) and (Mg2/Zn2) represent statistically distributed magnesium and zinc atoms with the atomic ratio close to 1:1.

The crystal structure can be described as an alternate stacking of V$_2$O$_7$ layers and (Mg/Zn) atom layers along [20$\bar{1}$] (Fig. 1*b*). Each V$_2$O$_7$ layer consists of two groups: a V$_2$O$_7$ dimer and a V$_4$O$_{14}$ tetramer. For illustration, a slab of one V$_2$O$_7$ layer and the adjacent (Mg/Zn) layer is shown in Fig. 1*c*,

Table 1
Experimental details.

Crystal data	
Chemical formula	MgZnV$_2$O$_7$
M_r	303.56
Crystal system, space group	Monoclinic, $C2/m$
Temperature (K)	298
a, b, c (Å)	10.32882 (7), 8.50126 (5), 9.30814 (6)
β (°)	98.5748 (5)
V (Å^3)	808.19 (1)
Z	6
Radiation type	Cu $K\alpha_1$, $\lambda = 1.5405$ Å
Specimen shape, size (mm)	Irregular, 24.9 × 24.9
Data collection	
Diffractometer	PANalytical Empyrean
Specimen mounting	Dispersed powder
Data collection mode	Reflection
Scan method	Step
2θ values (°)	$2\theta_{min} = 5.012$, $2\theta_{max} = 119.991$, $2\theta_{step} = 0.013$
Refinement	
R factors and goodness of fit	$R_p = 0.055$, $R_{wp} = 0.076$, $R_{exp} = 0.042$, $R(F^2) = 0.20886$, $\chi^2 = 3.276$
No. of parameters	40

Computer programs: *X'Pert Data Collector* and *X'Pert HighScore Plus* (PANalytical, 2011), *GSAS* (Larson & Von Dreele, 2000), *SHELXS97* (Sheldrick, 2008), *CRYSTALS* (Betteridge *et al.*, 2003) and *VESTA* (Momma & Izumi, 2011).

which is rotated by 90° from Fig. 1*b*. Two corner-sharing (V1)O$_4$ tetrahedra form the dimeric group. Two (V3)O$_4$ tetrahedra and two (V2)O$_5$ trigonal bipyramids form the tetrameric group, with a sequence of (V3)O$_4$–(V2)O$_5$–(V2)O$_5$–(V3)O$_4$. The two trigonal bipyramidal units in the middle are edge-sharing, each of which is corner-sharing with the adjacent terminal tetrahedron. (Mg1/Zn1) and (Mg2/Zn2) are coordinated by oxygen atoms in a distorted trigonal
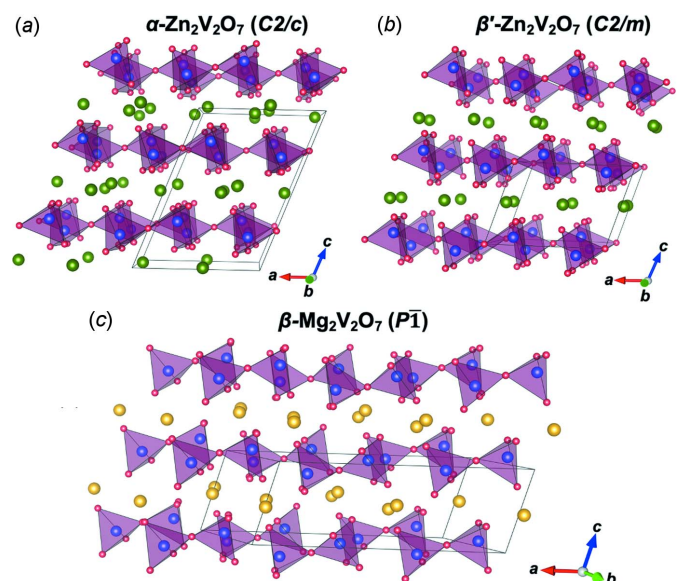

Figure 2
Crystal structure of (*a*) α-Zn$_2$V$_2$O$_7$, (*b*) thortveite-type β'-Zn$_2$V$_2$O$_7$, and (*c*) β-Mg$_2$V$_2$O$_7$.

bipyramidal and a distorted octahedral environment, respectively (Table 2).

The $MgZnV_2O_7$ structure ($C2/m$, $Z = 6$) is closely related to thortveitite-type α-$Zn_2V_2O_7$ ($C2/c$, $Z = 4$) (Gopal & Calvo, 1973), thortveite-type β'-$Zn_2V_2O_7$ ($C2/m$, $Z = 2$) (Krasnenko *et al.*, 2003), and β-$Mg_2V_2O_7$ ($P\bar{1}$, $Z = 2$) (Gopal & Calvo, 1974), as shown in Fig. 2, in which they have an alternate stacking of V_2O_7 layer and Zn or Mg layers. However, in contrast to $MgZnV_2O_7$, they only contain the V_2O_7 dimer groups. The relationships between other thortveitite-related phases are also well described in a previous work (Knowles *et al.*, 2018).

To check the refined structure model, empirical bond-valence sums (BVSs) were calculated (Brown & Altermatt, 1985; Brese & O'Keeffe, 1991), with the program *Valence* (Hormillosa *et al.*, 1993). The expected charges of the ions match the obtained BVS values (given in valence units): (Mg1/Zn1) = 1.96, (Mg2/Zn2) = 2.11, V1 = 6.08, V2 = 4.31, V3 = 4.69, O1 = 1.60, O2 = 2.26, O3 = 2.25, O4 = 1.71, O5 = 2.10, O6 = 1.87, O7 = 2.02, and O8 = 2.38. The high value for V1 comes from the relatively short V—O distances (Table 2). The restrained distance was slightly longer than the final values, however, the refinement led to the shorter distances. Short bond lengths (1.56–1.60 Å) were also found in other materials, such as $BiBa_2(VO_4)(V_2O_7)$ (Huang *et al.*, 1994) $Mg_2(V_2O_7)$ (Nielsen *et al.*, 2001) or $Th(V_2O_7)$ (Launay *et al.*, 1992). The final atomic positions were confirmed in the Fourier maps (observed and difference map).

3. Synthesis and crystallization

$MgZnV_2O_7$ was synthesized by a solid-state reaction from a mixture of $Mg(CH_3COO)_2 \cdot 4H_2O$ (98.0–102.0%, Alfa-Aesar), ZnO (99.99%, Aldrich) and V_2O_5 (99.99%, Aldrich) with a nominal composition of Mg:Zn:V = 1:1:2. The mixture was thoroughly ground in an agate mortar with acetone, dried, pressed into a pellet, heated in air at 673 K for 3 h, at 943 K for 6 h, and again at 1023 K for 6 h with intermediate grinding and pressing. For the powder X-ray diffraction measurement, the pellet was ground again in an agate mortar and the resultant powder was dispersed on a zero-background Si sample holder.

4. Refinement details

Details of the crystal data collection and structure refinement are summarized in Table 1 and the supporting information. Powder X-ray diffraction (PXRD) data for $MgZnV_2O_7$ were collected from a Bragg-Brentano diffractometer (PANalytical, 2011) using Cu $K\alpha_1$ radiation, a focusing primary Ge(111) monochromator (λ = 1.5405 Å) and a position-sensitive PIXcel 3D 2×2 detector. The angular range was set to $8° \leq 2\theta \leq 120°$, with a step of 0.0131° and a total measurement time of 8 h at room temperature. The PXRD pattern was indexed using the *DICVOL* algorithm (Boultif & Louër, 2004) run in *WINPLOT* (Roisnel & Rodríguez-Carvajal, 2000) through the positions of 26 reflections, resulting in a monoclinic unit cell (step 1). The space groups from the systematic reflection

Table 2
Selected bond lengths (Å).

Mg1—O3^i	1.975 (10)	V1—O3^{vii}	1.628 (10)
Mg1—O4^i	1.929 (9)	V1—O3^{viii}	1.628 (10)
Mg1—O5^{ii}	2.172 (10)	V1—O8	1.599 (15)
Mg1—O7^{iii}	2.081 (11)	V2—O1	1.959 (12)
Mg1—O8^{iii}	2.120 (11)	V2—O4	1.745 (9)
Mg2—O3^{iv}	2.354 (8)	V2—O4^{ix}	1.745 (9)
Mg2—O3^{ii}	2.354 (8)	V2—O7^x	2.032 (11)
Mg2—O5^v	1.948 (10)	V2—O7^{xi}	1.898 (15)
Mg2—O5^i	1.948 (10)	V3—O1^{xi}	1.824 (10)
Mg2—O6^{iii}	2.061 (10)	V3—O5^{xi}	1.703 (10)
Mg2—O6^{vi}	2.061 (10)	V3—O5^{xii}	1.703 (10)
V1—O2	1.757 (4)	V3—O6^{xi}	1.760 (15)

Symmetry codes: (i) $-x + \frac{1}{2}, y + \frac{1}{2}, -z + 1$; (ii) $x, -y + 1, z$; (iii) $x, y + 1, z$; (iv) $-x, -y + 1, -z + 1$; (v) $x - \frac{1}{2}, y + \frac{1}{2}, z$; (vi) $-x, y + 1, -z + 1$; (vii) $-x, y, -z + 1$; (viii) $-x, -y, -z + 1$; (ix) $x, -y, z$; (x) $x, y, z + 1$; (xi) $-x + 1, y, -z + 1$; (xii) $-x + 1, -y, -z + 1$.

conditions were suggested to be $C2/m$, $C2$, or Cm, which were indistinguishable from the reflection conditions. The highest symmetry, $C2/m$, was chosen first to determine the structure (step 2), and confirmed later. All the reflections were well indexed, except for a few minor unidentified impurity peaks. The structure determination was performed by a combination of the powder profile refinement program *GSAS* (Larson & Von Dreele, 2000) and the single-crystal structure-refinement program *CRYSTALS* (Betteridge *et al.*, 2003). The software *MCE* was used to visualize the three-dimensional Fourier electron-density maps, (Rohlíček & Hušák, 2007). Initially, a structural model was used with only one dummy atom placed at the (0,0,0) position in the unit cell. A Le Bail fit was used to extract the structure factors from the powder data in *GSAS* (step 3), followed by applying direct methods to build the initial structural solution, using *SHELXS97* (Sheldrick, 2008) run in *CRYSTALS*, which yielded three vanadium sites as the initial structural model (step 4). The initial dummy atom model was then replaced with the partial model containing
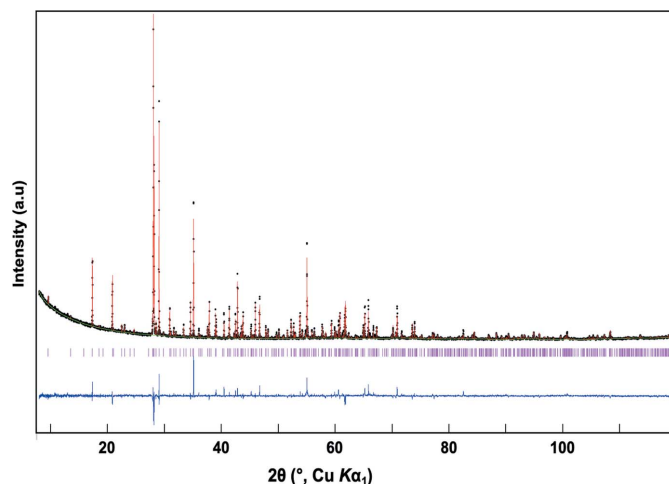

Figure 3
Powder X-ray diffraction Rietveld refinement profiles for $MgZnV_2O_7$ from room-temperature data. Black dots mark experimental data, the solid red line represents the calculated profile, and the solid green line is the background. The bottom trace presents the difference curve (blue) and the ticks denote the expected Bragg reflection positions (magenta).

only three vanadium atoms, and the Le Bail fit was applied in *GSAS* (step 5). Improved structure factors were then extracted, which were used for the refinement in *CRYSTALS* (step 6). This process (step 5 to 6) was repeated until a complete and satisfactory structural model was obtained. Finally, Rietveld refinement in *GSAS* was employed to complete the structure model, resulting in reasonable isotropic displacement parameters and agreement indices (step 7). The refinement parameters were scale factors, background, unit-cell parameters, peak profile coefficients, atomic coordinates, occupancies for the two (Mg/Zn) sites, common U_{iso} for the metal atoms, common U_{iso} for the oxygen atoms, and a March–Dollase preferential orientation coefficient (<111> direction). For the final Rietveld refinement cycles, the Mg—O, Zn—O, and V—O bond lengths were restrained with a tolerance value of 0.01 Å with respect to the distances determined from *CRYSTALS*, which matched reasonably well with the radii sums of Shannon (1976). Atomic coordinates and labeling were finally adapted from isotypic $Mn_{0.6}Zn_{1.4}V_2O_7$ (Knowles *et al.*, 2009). The final Rietveld plot is displayed in Fig. 3.

Acknowledgements

References

Betteridge, P. W., Carruthers, J. R., Cooper, R. I., Prout, K. & Watkin, D. J. (2003). *J. Appl. Cryst.* **36**, 1487.

Boultif, A. & Louër, D. (2004). *J. Appl. Cryst.* **37**, 724–731.

Brese, N. E. & O'Keeffe, M. (1991). *Acta Cryst.* B**47**, 192–197.

Brown, I. D. & Altermatt, D. (1985). *Acta Cryst.* B**41**, 244–247.

Chang, L. L. Y. & Wang, F. Y. (1988). *J. Am. Ceram. Soc.* **71**, 689–693.

Gopal, R. & Calvo, C. (1973). *Can. J. Chem.* **51**, 1004–1009.

Gopal, R. & Calvo, C. (1974). *Acta Cryst.* B**30**, 2491–2493.

Hormillosa, C., Healy, S., Stephen, T. & Brown, I. D. (1993). *Bond Valence Calculator.* Version 2.0. McMaster University, Canada.

Huang, J., Gu, Q. & Sleight, A. W. (1994). *J. Solid State Chem.* **110**, 226–233.

Knowles, K. M., Sil, A., Stöger, B. & Weil, M. (2018). *Acta Cryst.* C**74**, 1079–1087.

Knowles, K. M., Vickers, M. E., Sil, A., Han, Y.-H. & Jaffrenou, P. (2009). *Acta Cryst.* B**65**, 160–166.

Krasnenko, T. I., Zubkov, V. G. & Tjutinskaja, E. F. (2003). *Kristallografiya*, **48**, 40–43.

Larson, A. C. & Von Dreele, R. B. (2000). *General Structure Analysis System (GSAS).* Report LAUR. 86–748 Los Alamos National Laboratory, New Mexico, USA.

Launay, S., Mahe, P., Quarton, M. & Robert, F. (1992). *J. Solid State Chem.* **97**, 305–313.

Momma, K. & Izumi, F. (2011). *J. Appl. Cryst.* **44**, 1272–1276.

Nielsen, U. G., Jakobsen, H. J., Skibsted, J. & Norby, P. (2001). *J. Chem. Soc. Dalton Trans.* pp. 3214–3218.

PANalytical (2011). *X'Pert Data Collector and X'Pert High Score Plus.* PANalytical BV, Almelo, The Netherlands.

Rohlíček, J. & Hušák, M. (2007). *J. Appl. Cryst.* **40**, 600–601.

Roisnel, T. & Rodríguez-Carvajal, J. (2000). *WinPLOTR: a Windows tool for powder diffraction patterns analysis. Mater. Sci. Forum, Proc. 7th Europ. Powder Diff. Conf. (EPDIC 7)*, edited by R. Delhez & E. J. Mittenmeijer, pp. 118–123,

Shannon, R. D. (1976). *Acta Cryst.* A**32**, 751–767.

Sheldrick, G. M. (2008). *Acta Cryst.* A**64**, 112–122.

Crystal structure refinement of magnesium zinc divanadate, MgZnV$_2$O$_7$, from powder X-ray diffraction data

Stephanie J. Hong, Jun Li and Mas A. Subramanian

Computing details

Data collection: *X'Pert Data Collector* (PANalytical, 2011); cell refinement: *GSAS* (Larson & Von Dreele, 2000); data reduction: *X'Pert HighScore Plus* (PANalytical, 2011); program(s) used to solve structure: *SHELXS97* (Sheldrick, 2008) and *CRYSTALS* (Betteridge *et al.*, 2003); program(s) used to refine structure: *GSAS* (Larson & Von Dreele, 2000); molecular graphics: *VESTA* (Momma & Izumi, 2011); software used to prepare material for publication: *GSAS* (Larson & Von Dreele, 2000).

Magnesium zinc divanadate

Crystal data

MgZnV$_2$O$_7$	$V = 808.19$ (1) Å^3
$M_r = 303.56$	$Z = 6$
Monoclinic, $C2/m$	$F(000) = 864.0$
Hall symbol: -C 2y	$D_x = 3.743$ Mg m^{-3}
$a = 10.32882$ (7) Å	Cu $K\alpha_1$ radiation, $\lambda = 1.5405$ Å
$b = 8.50126$ (5) Å	$T = 298$ K
$c = 9.30814$ (6) Å	yellow
$\beta = 98.5748$ (5)°	irregular, 24.9 × 24.9 mm

Data collection

PANalytical Empyrean diffractometer	Specimen mounting: dispersed powder
Radiation source: sealed X-ray tube, PANalytical Cu Ceramic X-ray tube	Data collection mode: reflection
	Scan method: step
	$2\theta_{min} = 5.012°$, $2\theta_{max} = 119.991°$, $2\theta_{step} = 0.013°$

Refinement

Least-squares matrix: full

$R_p = 0.055$

$R_{wp} = 0.076$

$R_{exp} = 0.042$

$R(F^2) = 0.20886$

8758 data points

Excluded region(s): The background is too high at low angles and there was no Bragg's peaks.

Profile function: CW Profile function number 4 with 21 terms Pseudovoigt profile coefficients as parameterized in P. Thompson, D.E. Cox & J.B. Hastings (1987). J. Appl. Cryst.,20,79-83. Asymmetry correction of L.W. Finger, D.E. Cox & A. P. Jephcoat (1994). J. Appl. Cryst.,27,892-900. Microstrain broadening by P.W. Stephens, (1999). J. Appl. Cryst.,32,281-289. #1(GU) = 3.306 #2(GV) = 0.000 #3(GW) = 0.000 #4(GP) = 1.565 #5(LX) = 2.176 #6(ptec) = 0.00 #7(trns) = 0.00 #8(shft) = -0.5558 #9(sfec) = 0.00 #10(S/L) = 0.0005 #11(H/L) = 0.0005 #12(eta) = 0.7500 #13(S400) = 0.0E+00 #14(S040) = 0.0E+00 #15(S004) = 0.0E+00 #16(S220) = 0.0E+00 #17(S202) = 0.0E+00 #18(S022) = 0.0E+00 #19(S301) = 0.0E+00 #20(S103) = 0.0E+00 #21(S121) = 0.0E+00 Peak tails are ignored where the intensity is below 0.0020 times the peak Aniso. broadening axis 0.0 0.0 1.0

40 parameters

0 restraints

$(\Delta/\sigma)_{max} = 0.03$

Background function: GSAS Background function number 1 with 32 terms. Shifted Chebyshev function of 1st kind 1: 684.144 2: -705.826 3: 591.845 4: -383.442 5: 271.953 6: -144.446 7: 80.6035 8: -57.5987 9: 36.6287 10: -27.9916 11: 15.1285 12: -11.9775 13: 12.8819 14: -10.6721 15: 7.66251 16: -8.35018 17: 1.44025 18: -5.00721 19: 5.78817 20: -2.82870 21: 1.93935 22: -1.83947 23: 4.15929 24: 0.506732 25: -0.182215 26: 0.162584 27: 4.98669 28: 0.850932 29: -0.614188 30: -2.46723 31: 3.10631 32: 3.29784

Preferred orientation correction: March-Dollase AXIS 1 Ratio= 0.72861 h= 1.000 k= 1.000 l= 1.000 Prefered orientation correction range: Min= 0.62193, Max= 1.62737

Fractional atomic coordinates and isotropic or equivalent isotropic displacement parameters ($Å^2$)

	x	*y*	*z*	$U_{iso}*/U_{eq}$	Occ. (<1)
Mg1	0.3477 (3)	0.8175 (3)	0.2035 (3)	0.0069 (3)*	0.508 (4)
Mg2	0.0	0.8191 (5)	0.5	0.0069 (3)*	0.484 (7)
Zn1	0.3477 (3)	0.8175 (3)	0.2035 (3)	0.0069 (3)*	0.492 (4)
Zn2	0.0	0.8191 (5)	0.5	0.0069 (3)*	0.516 (7)
V1	0.0517 (4)	0.0	0.1885 (4)	0.0069 (3)*	
V2	0.3777 (4)	0.0	0.8892 (4)	0.0069 (3)*	
V3	0.6962 (4)	0.0	0.4938 (4)	0.0069 (3)*	
O1	0.4041 (12)	0.0	0.6850 (12)	0.0070 (8)*	
O2	0.0	0.0	0.0	0.0070 (8)*	
O3	0.0123 (9)	0.1586 (10)	0.7538 (9)	0.0070 (8)*	

O4	0.2787 (9)	0.1666 (10)	0.8864 (9)	0.0070 (8)*
O5	0.3613 (10)	0.1678 (11)	0.4382 (10)	0.0070 (8)*
O6	0.1338 (13)	0.0	0.5091 (13)	0.0070 (8)*
O7	0.4380 (14)	0.0	0.1072 (12)	0.0070 (8)*
O8	0.2081 (15)	0.0	0.2045 (13)	0.0070 (8)*

Geometric parameters (Å, º)

Mg1—Mg1[i]	3.104 (6)	V2—O1	1.959 (12)
Mg1—Mg2[ii]	3.185 (3)	V2—O4	1.745 (9)
Mg1—Zn1[i]	3.104 (6)	V2—O4[xv]	1.745 (9)
Mg1—Zn2[ii]	3.185 (3)	V2—O7[xvi]	2.032 (11)
Mg1—V3[iii]	3.307 (5)	V2—O7[xvii]	1.898 (15)
Mg1—O3[iv]	1.975 (10)	V3—Mg1[xviii]	3.307 (5)
Mg1—O4[iv]	1.929 (9)	V3—Mg1[xix]	3.307 (5)
Mg1—O5[v]	2.172 (10)	V3—O1[xvii]	1.824 (10)
Mg1—O7[vi]	2.081 (11)	V3—O5[xvii]	1.703 (10)
Mg1—O8[vi]	2.120 (11)	V3—O5[xx]	1.703 (10)
Mg2—Mg1[ii]	3.185 (3)	V3—O6[xvii]	1.760 (15)
Mg2—Mg1[vii]	3.185 (3)	O1—V2	1.959 (12)
Mg2—Mg2[viii]	3.076 (9)	O1—V3[xvii]	1.824 (10)
Mg2—Zn1[ii]	3.185 (3)	O2—V1	1.757 (4)
Mg2—Zn1[vii]	3.185 (3)	O2—V1[xxi]	1.757 (4)
Mg2—Zn2[viii]	3.076 (9)	O3—Mg1[xxii]	1.975 (10)
Mg2—O3[ix]	2.354 (8)	O3—Mg2[ix]	2.354 (8)
Mg2—O3[v]	2.354 (8)	O3—Zn1[xxii]	1.975 (10)
Mg2—O5[x]	1.948 (10)	O3—Zn2[ix]	2.354 (8)
Mg2—O5[iv]	1.948 (10)	O3—V1[xii]	1.628 (10)
Mg2—O6[vi]	2.061 (10)	O4—Mg1[xxii]	1.929 (9)
Mg2—O6[xi]	2.061 (10)	O4—Zn1[xxii]	1.929 (9)
Zn1—Mg1[i]	3.104 (6)	O4—V2	1.745 (9)
Zn1—Mg2[ii]	3.185 (3)	O5—Mg1[v]	2.172 (10)
Zn1—Zn1[i]	3.104 (6)	O5—Mg2[xxiii]	1.948 (10)
Zn1—O3[iv]	1.975 (10)	O5—Zn1[v]	2.172 (10)
Zn1—O4[iv]	1.929 (9)	O5—Zn2[xxiii]	1.948 (10)
Zn1—O5[v]	2.172 (10)	O5—V3[xvii]	1.703 (10)
Zn1—O7[vi]	2.081 (11)	O6—Mg2[xxiv]	2.061 (10)
Zn1—O8[vi]	2.120 (11)	O6—Mg2[ix]	2.061 (10)
Zn2—Mg1[ii]	3.185 (3)	O6—Zn2[xxiv]	2.061 (10)
Zn2—Mg1[vii]	3.185 (3)	O6—Zn2[ix]	2.061 (10)
Zn2—Mg2[viii]	3.076 (9)	O6—V3[xvii]	1.760 (15)
Zn2—Zn2[viii]	3.076 (9)	O7—Mg1[xxiv]	2.081 (11)
Zn2—O3[ix]	2.354 (8)	O7—Mg1[v]	2.081 (11)
Zn2—O3[v]	2.354 (8)	O7—Zn1[xxiv]	2.081 (11)
Zn2—O5[x]	1.948 (10)	O7—Zn1[v]	2.081 (11)
Zn2—O5[iv]	1.948 (10)	O7—V2[xxv]	2.032 (11)
Zn2—O6[vi]	2.061 (10)	O7—V2[xvii]	1.898 (15)
Zn2—O6[xi]	2.061 (10)	O8—Mg1[xxiv]	2.120 (11)

V1—O2	1.757 (4)	O8—Mg1ᵛ	2.120 (11)
V1—O3ˣⁱⁱ	1.628 (10)	O8—Zn1ˣˣⁱᵛ	2.120 (11)
V1—O3ˣⁱⁱⁱ	1.628 (10)	O8—Zn1ᵛ	2.120 (11)
V1—O8	1.599 (15)	O8—V1	1.599 (15)
V2—V2ˣⁱᵛ	3.014 (6)		
Mg1ⁱ—Mg1—Mg2ⁱⁱ	111.37 (6)	O3ˣⁱⁱ—V1—O3ˣⁱⁱⁱ	111.9 (8)
Mg1ⁱ—Mg1—O3ⁱᵛ	133.1 (3)	O3ˣⁱⁱ—V1—O8	115.1 (4)
Mg1ⁱ—Mg1—O4ⁱᵛ	131.7 (3)	O3ˣⁱⁱⁱ—V1—O8	115.1 (4)
Mg1ⁱ—Mg1—O5ᵛ	86.7 (2)	O1—V2—O4	98.7 (4)
Mg1ⁱ—Mg1—O7ᵛⁱ	41.8 (3)	O1—V2—O4ˣᵛ	98.7 (4)
Mg1ⁱ—Mg1—O8ᵛⁱ	42.9 (3)	O1—V2—O7ˣᵛⁱ	154.4 (6)
Mg2ⁱⁱ—Mg1—O3ⁱᵛ	47.5 (3)	O1—V2—O7ˣᵛⁱⁱ	74.5 (5)
Mg2ⁱⁱ—Mg1—O4ⁱᵛ	110.4 (3)	O4—V2—O4ˣᵛ	108.5 (7)
Mg2ⁱⁱ—Mg1—O5ᵛ	36.9 (3)	O4—V2—O7ˣᵛⁱ	96.1 (4)
Mg2ⁱⁱ—Mg1—O7ᵛⁱ	116.7 (3)	O4—V2—O7ˣᵛⁱⁱ	125.7 (3)
Mg2ⁱⁱ—Mg1—O8ᵛⁱ	120.7 (4)	O4ˣᵛ—V2—O7ˣᵛⁱ	96.1 (4)
O3ⁱᵛ—Mg1—O4ⁱᵛ	93.5 (3)	O4ˣᵛ—V2—O7ˣᵛⁱⁱ	125.7 (3)
O3ⁱᵛ—Mg1—O5ᵛ	84.3 (3)	O7ˣᵛⁱ—V2—O7ˣᵛⁱⁱ	79.9 (7)
O3ⁱᵛ—Mg1—O7ᵛⁱ	103.6 (5)	O1ˣᵛⁱⁱ—V3—O5ˣᵛⁱⁱ	99.1 (4)
O3ⁱᵛ—Mg1—O8ᵛⁱ	167.9 (4)	O1ˣᵛⁱⁱ—V3—O5ˣˣ	99.1 (4)
O4ⁱᵛ—Mg1—O5ᵛ	114.4 (4)	O1ˣᵛⁱⁱ—V3—O6ˣᵛⁱⁱ	114.7 (7)
O4ⁱᵛ—Mg1—O7ᵛⁱ	128.8 (4)	O5ˣᵛⁱⁱ—V3—O5ˣˣ	113.8 (8)
O4ⁱᵛ—Mg1—O8ᵛⁱ	94.1 (4)	O5ˣᵛⁱⁱ—V3—O6ˣᵛⁱⁱ	114.2 (4)
O5ᵛ—Mg1—O7ᵛⁱ	115.1 (4)	O5ˣˣ—V3—O6ˣᵛⁱⁱ	114.2 (4)
O5ᵛ—Mg1—O8ᵛⁱ	84.0 (5)	V2—O1—V3ˣᵛⁱⁱ	138.0 (7)
O7ᵛⁱ—Mg1—O8ᵛⁱ	78.8 (4)	V1—O2—V1ˣˣⁱ	180.0
Mg1ⁱⁱ—Mg2—Mg1ᵛⁱⁱ	137.26 (13)	Mg1ˣˣⁱⁱ—O3—Mg2ⁱˣ	94.3 (4)
Mg1ⁱⁱ—Mg2—Mg2ᵛⁱⁱⁱ	111.37 (6)	Mg1ˣˣⁱⁱ—O3—Zn1ˣˣⁱⁱ	0.0
Mg1ⁱⁱ—Mg2—O3ⁱˣ	147.6 (2)	Mg1ˣˣⁱⁱ—O3—V1ˣⁱⁱ	145.2 (5)
Mg1ⁱⁱ—Mg2—O3ᵛ	38.2 (2)	Mg2ⁱˣ—O3—Zn1ˣˣⁱⁱ	94.3 (4)
Mg1ⁱⁱ—Mg2—O5ˣ	105.2 (3)	Mg2ⁱˣ—O3—V1ˣⁱⁱ	115.7 (4)
Mg1ⁱⁱ—Mg2—O5ⁱᵛ	42.0 (3)	Zn1ˣˣⁱⁱ—O3—V1ˣⁱⁱ	145.2 (5)
Mg1ⁱⁱ—Mg2—O6ᵛⁱ	89.7 (3)	Mg1ˣˣⁱⁱ—O4—Zn1ˣˣⁱⁱ	0.0
Mg1ⁱⁱ—Mg2—O6ˣⁱ	123.3 (3)	Mg1ˣˣⁱⁱ—O4—V2	154.6 (5)
Mg1ᵛⁱⁱ—Mg2—Mg2ᵛⁱⁱⁱ	111.37 (6)	Zn1ˣˣⁱⁱ—O4—V2	154.6 (5)
Mg1ᵛⁱⁱ—Mg2—O3ⁱˣ	38.2 (2)	Mg1ᵛ—O5—Mg2ˣˣⁱⁱⁱ	101.1 (5)
Mg1ᵛⁱⁱ—Mg2—O3ᵛ	147.6 (2)	Mg1ᵛ—O5—Zn1ᵛ	0.0
Mg1ᵛⁱⁱ—Mg2—O5ˣ	42.0 (3)	Mg1ᵛ—O5—Zn2ˣˣⁱⁱⁱ	101.1 (5)
Mg1ᵛⁱⁱ—Mg2—O5ⁱᵛ	105.2 (3)	Mg1ᵛ—O5—V3ˣᵛⁱⁱ	116.7 (5)
Mg1ᵛⁱⁱ—Mg2—O6ᵛⁱ	123.3 (3)	Mg2ˣˣⁱⁱⁱ—O5—Zn1ᵛ	101.1 (5)
Mg1ᵛⁱⁱ—Mg2—O6ˣⁱ	89.7 (3)	Mg2ˣˣⁱⁱⁱ—O5—Zn2ˣˣⁱⁱⁱ	0.0
Mg2ᵛⁱⁱⁱ—Mg2—O3ⁱˣ	85.4 (2)	Mg2ˣˣⁱⁱⁱ—O5—V3ˣᵛⁱⁱ	136.5 (5)
Mg2ᵛⁱⁱⁱ—Mg2—O3ᵛ	85.4 (2)	Zn1ᵛ—O5—Zn2ˣˣⁱⁱⁱ	101.1 (5)
Mg2ᵛⁱⁱⁱ—Mg2—O5ˣ	131.3 (3)	Zn1ᵛ—O5—V3ˣᵛⁱⁱ	116.7 (5)
Mg2ᵛⁱⁱⁱ—Mg2—O5ⁱᵛ	131.3 (3)	Zn2ˣˣⁱⁱⁱ—O5—V3ˣᵛⁱⁱ	136.5 (5)
Mg2ᵛⁱⁱⁱ—Mg2—O6ᵛⁱ	41.7 (3)	Mg2ˣˣⁱᵛ—O6—Mg2ⁱˣ	96.5 (6)
Mg2ᵛⁱⁱⁱ—Mg2—O6ˣⁱ	41.7 (3)	Mg2ˣˣⁱᵛ—O6—Zn2ˣˣⁱᵛ	0.0

O3^{ix}—Mg2—O3^{v}	170.8 (4)	Mg2^{xxiv}—O6—Zn2^{ix}	96.5 (6)
O3^{ix}—Mg2—O5^{x}	80.2 (3)	Mg2^{xxiv}—O6—V3^{xvii}	131.6 (3)
O3^{ix}—Mg2—O5^{iv}	106.1 (4)	Mg2^{ix}—O6—Zn2^{xxiv}	96.5 (6)
O3^{ix}—Mg2—O6^{vi}	85.2 (4)	Mg2^{ix}—O6—Zn2^{ix}	0.0
O3^{ix}—Mg2—O6^{xi}	87.9 (4)	Mg2^{ix}—O6—V3^{xvii}	131.6 (3)
O3^{v}—Mg2—O5^{x}	106.1 (4)	Zn2^{xxiv}—O6—Zn2^{ix}	96.5 (6)
O3^{v}—Mg2—O5^{iv}	80.2 (3)	Zn2^{xxiv}—O6—V3^{xvii}	131.6 (3)
O3^{v}—Mg2—O6^{vi}	87.9 (4)	Zn2^{ix}—O6—V3^{xvii}	131.6 (3)
O3^{v}—Mg2—O6^{xi}	85.2 (4)	Mg1^{xxiv}—O7—Mg1^{v}	96.4 (6)
O5^{x}—Mg2—O5^{iv}	97.3 (5)	Mg1^{xxiv}—O7—Zn1^{xxiv}	0.0
O5^{x}—Mg2—O6^{vi}	164.7 (4)	Mg1^{xxiv}—O7—Zn1^{v}	96.4 (6)
O5^{x}—Mg2—O6^{xi}	91.2 (4)	Mg1^{xxiv}—O7—V2^{xxv}	109.8 (4)
O5^{iv}—Mg2—O6^{vi}	91.2 (4)	Mg1^{xxiv}—O7—V2^{xvii}	120.3 (4)
O5^{iv}—Mg2—O6^{xi}	164.7 (4)	Mg1^{v}—O7—Zn1^{xxiv}	96.4 (6)
O6^{vi}—Mg2—O6^{xi}	83.5 (6)	Mg1^{v}—O7—Zn1^{v}	0.0
O3^{iv}—Zn1—O4^{iv}	93.5 (3)	Mg1^{v}—O7—V2^{xxv}	109.8 (4)
O3^{iv}—Zn1—O5^{v}	84.3 (3)	Mg1^{v}—O7—V2^{xvii}	120.3 (4)
O3^{iv}—Zn1—O7^{vi}	103.6 (5)	Zn1^{xxiv}—O7—Zn1^{v}	96.4 (6)
O3^{iv}—Zn1—O8^{vi}	167.9 (4)	Zn1^{xxiv}—O7—V2^{xxv}	109.8 (4)
O4^{iv}—Zn1—O5^{v}	114.4 (4)	Zn1^{xxiv}—O7—V2^{xvii}	120.3 (4)
O4^{iv}—Zn1—O7^{vi}	128.8 (4)	Zn1^{v}—O7—V2^{xxv}	109.8 (4)
O4^{iv}—Zn1—O8^{vi}	94.1 (4)	Zn1^{v}—O7—V2^{xvii}	120.3 (4)
O5^{v}—Zn1—O7^{vi}	115.1 (4)	V2^{xxv}—O7—V2^{xvii}	100.1 (7)
O5^{v}—Zn1—O8^{vi}	84.0 (5)	Mg1^{xxiv}—O8—Mg1^{v}	94.1 (7)
O7^{vi}—Zn1—O8^{vi}	78.8 (4)	Mg1^{xxiv}—O8—Zn1^{xxiv}	0.0
O5^{x}—Zn2—O5^{iv}	97.3 (5)	Mg1^{xxiv}—O8—Zn1^{v}	94.1 (7)
O5^{x}—Zn2—O6^{vi}	164.7 (4)	Mg1^{xxiv}—O8—V1	132.7 (3)
O5^{x}—Zn2—O6^{xi}	91.2 (4)	Mg1^{v}—O8—Zn1^{xxiv}	94.1 (7)
O5^{iv}—Zn2—O6^{vi}	91.2 (4)	Mg1^{v}—O8—Zn1^{v}	0.0
O5^{iv}—Zn2—O6^{xi}	164.7 (4)	Mg1^{v}—O8—V1	132.7 (3)
O6^{vi}—Zn2—O6^{xi}	83.5 (6)	Zn1^{xxiv}—O8—Zn1^{v}	94.1 (7)
O2—V1—O3^{xii}	104.6 (3)	Zn1^{xxiv}—O8—V1	132.7 (3)
O2—V1—O3^{xiii}	104.6 (3)	Zn1^{v}—O8—V1	132.7 (3)
O2—V1—O8	104.2 (5)		

Symmetry codes: (i) x, $-y+2$, z; (ii) $-x+1/2$, $-y+3/2$, $-z+1$; (iii) $-x+1$, $y+1$, $-z+1$; (iv) $-x+1/2$, $y+1/2$, $-z+1$; (v) x, $-y+1$, z; (vi) x, $y+1$, z; (vii) $x-1/2$, $-y+3/2$, z; (viii) $-x$, $-y+2$, $-z+1$; (ix) $-x$, $-y+1$, $-z+1$; (x) $x-1/2$, $y+1/2$, z; (xi) $-x$, $y+1$, $-z+1$; (xii) $-x$, y, $-z+1$; (xiii) $-x$, $-y$, $-z+1$; (xiv) $-x+1$, y, $-z+2$; (xv) x, $-y$, z; (xvi) x, y, $z+1$; (xvii) $-x+1$, y, $-z+1$; (xviii) $-x+1$, $y-1$, $-z+1$; (xix) $-x+1$, $-y+1$, $-z+1$; (xx) $-x+1$, $-y$, $-z+1$; (xxi) $-x$, y, $-z$; (xxii) $-x+1/2$, $y-1/2$, $-z+1$; (xxiii) $x+1/2$, $y-1/2$, z; (xxiv) x, $y-1$, z; (xxv) x, y, $z-1$.